Quantum Chemical Study of Ion−Molecule Reactions in $N_2^+ + O_2$ System

Akitomo Tachibana,*,† Koichi Nakamura,‡ Tasuku Yano,‡ Yoichi Sugiyama,‡ and Shogo Tanimura†

Department of Engineering Physics and Mechanics, Kyoto University, Kyoto, 606-8501, Japan, and Department of Molecular Engineering, Kyoto University, Kyoto, 606-8501, Japan

Received: September 1, 1998; In Final Form: February 1, 1999

We report a study of the ab initio quantum chemical calculations for an ion−molecule reaction in the $N_2^+ + O_2$ system at the CCSD(T)/6-31G*//MP2(full)/6-31G* level augmented by multireference configuration interaction (MRCI) calculations. For the charge transfer (CT) reaction $N_2^+ + O_2 \rightarrow N_2 + O_2^+$, different mechanisms of electron transfer exist according to the electronic state of N_2^+. Along the potential energy curve with C_{2v} symmetry, electron transfer to $N_2^+(X^2\Sigma_g^+)$ occurs via a quartet T-shaped intermediate complex where positive charge has already been distributed on the O_2 fragment, and the CT leads to $O_2^+(a^4\Pi_u)$ with large endothermicity. In contrast, electron transfer to $N_2^+(A^2\Pi_u)$ occurs via a doublet T-shaped intermediate complex, and the CT leads to $O_2^+(X^2\Pi_g)$ with large exothermicity. The doublet and quartet energy surfaces that connect the reactant systems, the intermediate complexes, and the product systems are examined in detail. The quartet CT reaction path contributes to the vibrational deactivation of $N_2^+(X^2\Sigma_g^+)$. Related characteristics of the reaction dynamics are also discussed.

Introduction

Ion−molecule reactions have been of central interest in the chemistry of the ionosphere.[1] Not only in the basic study of earth's upper atmosphere but also from the fundamental interest in state-to-state chemistry, the ion−molecule reaction between the nitrogen molecule cation N_2^+ and oxygen molecule O_2 has received considerable attention, and many experimental studies have been carried out in order to clarify the reaction mechanism.[2−9] For this reaction system, the charge transfer (CT) reaction

$$N_2^+(X^2\Sigma_g^+,A^2\Pi_u;v) + O_2(X^3\Sigma_g^-) \rightarrow N_2(X^1\Sigma_g^+;v') + O_2^+(X^2\Pi_g,a^4\Pi_u;v'') \quad (1)$$

is a main channel of the reaction pathways. The vibrational excitation of ions can significantly alter the reaction pathways, the electronic species, the vibrational states of products, and the rate constants.[2−12]

Koyano et al. were the first to report the effect of vibrational excitation of N_2^+ on CT reaction 1 using the photoelectron−photoion coincidence (PEPICO) technique.[2] They selected vibrational states of $N_2^+(X^2\Sigma_g^+;v=0-3)$ and $N_2^+(A^2\Pi_u;v=0-3)$ at considerably high collision energy, $E_{CM} = 2.1$ eV, and found that the cross section of the CT reaction for $N_2^+(X^2\Sigma_g^+;v)$ was very small compared with that for $N_2^+(A^2\Pi_u;v)$ and almost unaffected by the stretching vibrational quantum number v. If the $O_2^+(a^4\Pi_u)$ product ion is obtained from the $N_2^+(X^2\Sigma_g^+;v) + O_2(X^3\Sigma_g^-)$ reactant system by the CT reaction, it seems that the cross section of this reaction would show the vibrational enhancement from the viewpoint of energetics; the energy level of the $N_2(X^1\Sigma_g^+;v'=0) + O_2^+(a^4\Pi_u;v''=0)$ product state is 0.523 eV above the ground state $v = 0$ of the reactant, while the vibrationally excited reactant states are 0.270 eV ($v = 1$), 0.535 eV ($v = 2$), 0.797 eV ($v = 3$), and 1.054 eV ($v = 4$), respectively.[13] Indeed, the reverse reaction of CT reaction 1, $O_2^+(a^4\Pi_u) + N_2(X^1\Sigma_g^+) \rightarrow O_2(X^3\Sigma_g^-) + N_2^+(X^2\Sigma_g^+)$, occurs with high probability,[10] which implies that the reaction pathway connecting the $N_2^+(X^2\Sigma_g^+) + O_2(X^3\Sigma_g^-)$ state and the $N_2(X^1\Sigma_g^+) + O_2^+(a^4\Pi_u)$ state should exist. Therefore, it appears that the $N_2^+(X^2\Sigma_g^+;v) + O_2(X^3\Sigma_g^-)$ reactant system may lead to $O_2^+(a^4\Pi_u)$ by the CT reaction 1 with high energy. Koyano et al. inferred that the product of the CT reaction from $N_2^+(X^2\Sigma_g^+)$ was not $O_2^+(a^4\Pi_u)$ but $O_2^+(X^2\Pi_g)$, since the vibrational enhancement of the CT reaction for $N_2^+(X^2\Sigma_g^+;v)$ was not observed.[2] On the other hand, they concluded that the vibrational enhancement of the CT reaction for $N_2^+(A^2\Pi_u;v)$ was observed.[2]

Ferguson et al. proposed the "T"-shaped complex of $N_2^+ + O_2$ system,[3] which is drawn in Figure 3, as an intermediate state of the CT reaction and predicted the electronic structure of the product O_2 in terms of the molecular orbital (MO) overlapping feasibility. In the T-shaped complex, the $3\sigma_g$ singly occupied molecular orbital (SOMO) of $N_2^+(X^2\Sigma_g^+)$ has an in-phase overlap with the $1\pi_u$ orbital of $O_2(X^3\Sigma_g^-)$ whose removal leads to $O_2^+(a^4\Pi_u)$, while the overlap between the $3\sigma_g$ orbital of $N_2^+(X^2\Sigma_g^+)$ and the $1\pi_g$ orbital of $O_2(X^3\Sigma_g^-)$, whose removal leads to $O_2^+(X^2\Pi_g)$, is zero by symmetry. Therefore, they inferred the product of the CT reaction from $N_2^+(X^2\Sigma_g^+)$ was endothermic leading to $O_2^+(a^4\Pi_u)$, and this inference was supported by the fact that the rate constant of the CT reaction, k_{CT}, from $N_2^+(X^2\Sigma_g^+)$ was extraordinarily small: $k_{CT} \approx 5 \times 10^{-11}$ cm^3 s^{-1}.[3−9]

Schultz and Armentrout studied the reaction of $N_2^+(X^2\Sigma_g^+)$ with $O_2(X^3\Sigma_g^-)$ under single-collision conditions in a guided-ion beam mass spectrometer at $E_{CM} = 0.04-20$ eV.[4] The observed cross section of the CT reaction 1 for the $N_2^+(X^2\Sigma_g^+) + O_2(X^3\Sigma_g^-)$ reactant system was much smaller than the theoretical value; the observed cross section was about 15% ± 8% of the calculated value by the Langevin−Gioumousis−Stevenson (LGS) expression,[14] despite exothermicity of 3.509

† Department of Engineering Physics and Mechanics.
‡ Department of Molecular Engineering.

10.1021/jp983578s CCC: $18.00
Published on Web 06/26/1999

eV.[13] Moreover, the CT cross section also indicated an unusual dependence on the collision energy E_{CM}; as E_{CM} increases, the CT cross section decreases until E_{CM} reaches 1 eV and exhibits the minimum at $E_{CM} = 1$ eV and increases when E_{CM} exceeds 1 eV. If E_{CM} increases more, the CT cross section exhibits a local maximum and then decreases again.[4] The rate constant of the CT reaction 1 for the $N_2^+(X^2\Sigma_g^+) + O_2(X^3\Sigma_g^-)$ reactant system also exhibits the minimum with respect to the collision energy near 1 eV.[5] Schultz and Armentrout explained both the smallness and complicated energy dependence of the observed CT cross section by means of the long-range direct mechanism, which is driven by the Franck−Condon (FC) factors.[11,15] In reaction 1 for the $N_2^+(X^2\Sigma_g^+;v) + O_2(X^3\Sigma_g^-)$ reactant system, there is no resonant state of $O_2^+(X^2\Pi_g)$ at the ionization energy of $N_2(X^1\Sigma_g^+)$, and moreover, the FC factors are too small to produce $O_2^+(X^2\Pi_g)$ efficiently. Therefore, the small CT cross section is observed. As E_{CM} increases, the system is separated far from the resonance states of $O_2^+(X^2\Pi_g)$, and when E_{CM} exceeds ca. 1 eV, the FC factors might begin to associate with the $O_2^+(a^4\Pi_u)$ band. According to the FC criteria for a long-range vertical transition, the product state is not $O_2^+(a^4\Pi_u;v''=0)$, which corresponds to the adiabatic ionization of O_2, but $O_2^+(a^4\Pi_u;v''=4)$,[16] where the vertical ionization is most enhanced at $E_{CM} = 1.011$ eV.[13] Among the vibrational states of product $N_2(X^1\Sigma_g^+)$ the state $v' = 0$ is produced with large probability, since the $N_2^+(X^2\Sigma_g^+) \rightarrow N_2(X^1\Sigma_g^+)$ transition is almost vertical and keeps the vibrational quantum number $v' = v$ well. Therefore, the CT cross section increases when E_{CM} exceeds 1 eV by opening of the $O_2^+(a^4\Pi_u)$ formation channel. In the experiments by Koyano et al.,[2] CT reaction 1 might be dominated by the long-range direct process because of the large collision energy of 2.1 eV. As Schultz and Armentrout pointed out,[4] the $N_2^+(X^2\Sigma_g^+;v=0)$ state might already couple with the $O_2^+(a^4\Pi_u)$ product state if $E_{CM} = 2.1$ eV is efficiently channeled into the reaction coordinate. Then it is not surprising that the results by Koyano et al. did not indicate a vibrational enhancement in CT reaction 1 for $N_2^+(X^2\Sigma_g^+)$ because the translational energy contributes to open the $O_2^+(a^4\Pi_u)$ channel more than the vibrational energy of $N_2^+(X^2\Sigma_g^+)$.

Recently, Kato et al. studied the vibrational dependence of the short-range CT reaction 1 for the $N_2^+(X^2\Sigma_g^+;v)$ state using the selected-ion flow tube, laser-induced fluorescence (SIFT-LIF) technique for $v = 0-4$ at very small translational energies, where translational enhancement was negligible, and suggested a reaction mechanism involving short-range interaction via an ion−molecule intermediate complex.[6,7] In the short-range interaction, the FC mechanism will be unqualified and the adiabatic ionization to $O_2^+(a^4\Pi_u;v''=0)$ might be adapted. Above all, the $N_2^+(X^2\Sigma_g^+;v=2)$ state (0.535 eV) is almost exactly resonant with the $O_2^+(a^4\Pi_u;v''=0)$ product state (0.523 eV), and hence, a large dependency on the vibrational state for CT is expected. At the beginning of their study for $v \leq 2$, the vibrational enhancement of the CT reaction 1 was regarded as negligibly small because the CT rate constants are almost constant for $v \leq 2$ if the data of N_2^+ ion counts detected with the downstream mass filter as a function of O_2 flow rate are treated as a single-exponential decay: $k_{CT,0} = k_{CT,1} = k_{CT,2} = 0.49 \times 10^{-10}$ cm^3 s^{-1} for $v = 0$, 1, and 2, but a CT enhancement of ca. 50% for $v = 2$ was suggested if the slight curvature of the data of N_2^+ ion counts is fit exactly.[6] By means of the latest analysis of experimental kinetic plots, a moderate CT enhancement of ca. 50% for $v \geq 2$ is observed with the improved LIF measurements.[7] For the low vibrational state for $v < 2$, it has been considered that the endothermicity due to the small vibrational energy makes the CT avoid accessing the $O_2^+(a^4\Pi_u)$ state, and in the case of coupling with the $O_2^+(X^2\Pi_g)$ state, the vibrational enhancement is not observed because of the high exothermicity.

Simultaneously, Kato et al. investigated the vibrational deactivation reaction

$$N_2^+(X^2\Sigma_g^+;v>0) + O_2(X^3\Sigma_g^-) \rightarrow N_2^+(v'<v) + O_2 \quad (2)$$

at low E_{CM}.[6,7] This reaction occurs in competition with CT reaction 1. They investigated the rate constants of vibrational relaxation k_q for $v = 1-4$ by means of the latest analysis of experimental kinetics plots considering the multiquantum deactivations, and a significant enhancement of vibrational deactivation was observed; the total rate constants $k_{CT} + k_q$, whose enhancement is primarily due to increased vibrational deactivation, are 0.49×10^{-10}, 1.6×10^{-10}, 2.1×10^{-10}, 2.6×10^{-10}, and 3.0×10^{-10} cm^3 s^{-1} for $v = 0$, 1, 2, 3, and 4, respectively; that is, the total rate constant for $v = 4$ is 6 times larger than that for $v = 0$.[7] The properties that neither N_2^+ nor O_2 has a permanent dipole moment and that the vibrational levels between N_2^+ and O_2 have a large gap for energy defect would hamper the long-range direct vibration-to-vibration energy transfer from $N_2^+(v)$ to O_2. Therefore, they suggested that reaction 2 also occurs via a short-range mechanism, in the $(N_2^+\cdot\cdot\cdot O_2)$ intermediate complex, which has a deep potential well due to an electron exchange, on the CT reaction path, and estimated effective well depths of 0.8, 0.9, and 1.0 eV for the $N_2^+(^2\Sigma_g^+;v=0)$, $N_2^+(^2\Sigma_g^+;v=1)$, and $N_2^+(^2\Sigma_g^+;v=2)$ reactants, respectively, when a moderate exchange integral for the electronic coupling between $N_2^+(^2\Sigma_g^+) + O_2(^3\Sigma_g^-)$ reactant system and $N_2(^1\Sigma_g^+) + O_2^+(^4\Pi_u)$ product system was assumed to be 0.8 eV.[6,7] For this reactant system, Dobler et al. investigated the kinetic energy dependence of k_q;[8] they observed that k_q was almost independent of E_{CM}, although k_q exhibited a slight minimum around $E_{CM} = 0.5$ eV. They regarded that the slight decrease of k_q was due to the reduction of the lifetime of the intermediate complex.

Moreover, Schultz and Armentrout observed first that the abstraction reactions also occur at higher collision energies for this system as well as for the $(N_2 + H_2)^+$ or $(O_2 + H_2)^+$ system as follows:[4]

$$N_2^+(X^2\Sigma_g^+) + O_2(X^3\Sigma_g^-) \rightarrow N_2O^+(X^2\Pi, {}^4A'', {}^4\Sigma^-) + O(^3P) \quad (3)$$

$$N_2^+(X^2\Sigma_g^+) + O_2(X^3\Sigma_g^-) \rightarrow NO^+(X^1\Sigma^+) + N(^4S, {}^2D) + O(^3P) \quad (4)$$

$$N_2^+(X^2\Sigma_g^+) + O_2(X^3\Sigma_g^-) \rightarrow O^+(^4S) + N_2(X^1\Sigma_g^+) + O(^3P) \quad (5)$$

It has been reported that NO_2^+ and NO_2 are not observed as the product species. They suggested an intermediate of the form $(N-N\cdots O-O)^+$, which should have a doublet ground state corresponding to covalent bond formation between N_2 and O_2 fragments, where the N−N cleavage is hard to occur. In reaction 3 the ground state of N_2O^+ is $^2\Pi$, while reactions 4 and 5 are respectively derived from the excited $^4A''$ state and $^4\Sigma^-$ state of N_2O^+ with conserving spin symmetry.[4,17,18] The surface crossing has been discussed in the dissociation of $N_2O^+(^2\Pi)$ to $NO^+(X^1\Sigma^+) + N(^4S)$ or $O^+(^4S) + N_2(X^1\Sigma_g^+)$.[17]

It is essential for discussion of the vibrational effects to investigate detailed reaction mechanisms and potential energy

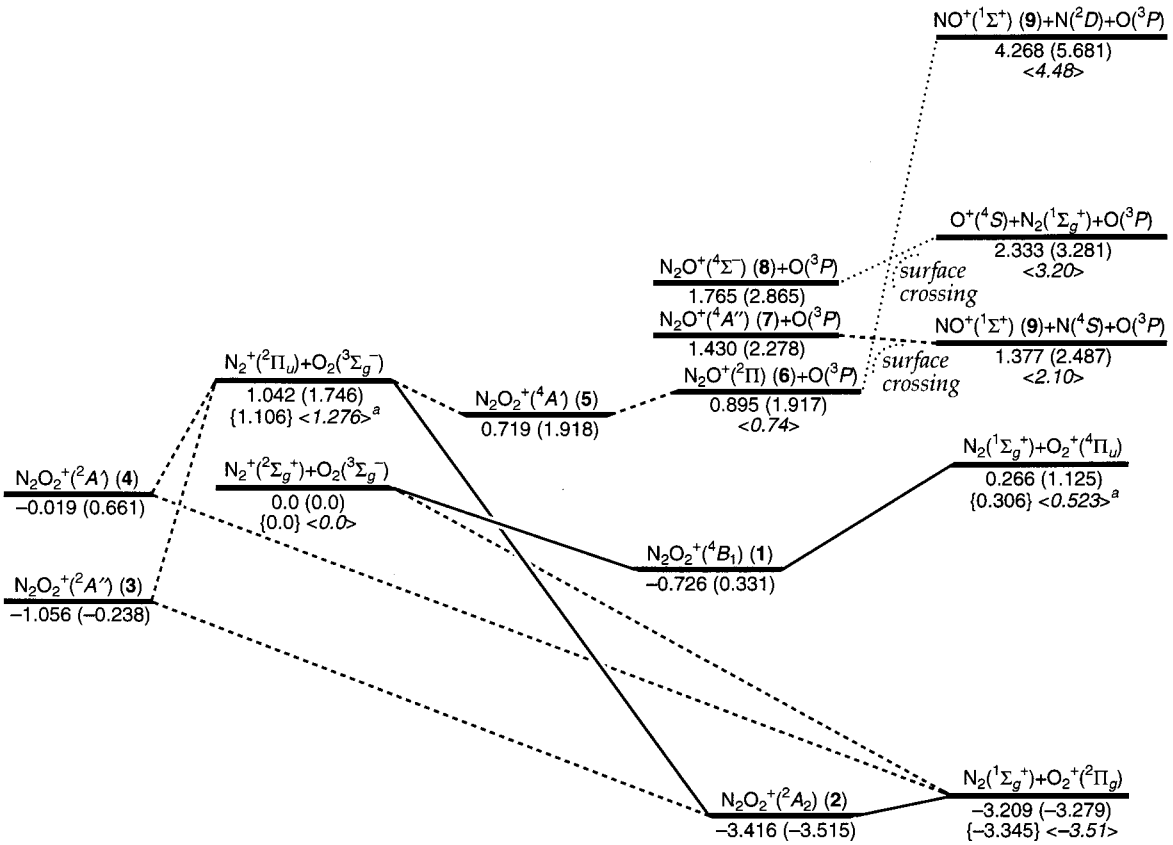

Figure 1. Electronic state correlation diagram of $N_2^+ + O_2$ system at the CCSD(T)/6-31G*//UMP2(full)/6-31G* level with ZPE correction at the MP2 level in units of electronvolt. Solid lines, dashed lines, and dotted lines indicate the potential energy surfaces with maintained symmetries of C_{2v}, C_s, and $C_{\infty v}$, respectively. Values in parentheses are relative energies at the PMP2(full)/6-31G*+ZPE level. Results of MRCI calculations are in brackets. Values in brackets are experimental data in ref 4 except *a* from ref 6.

surfaces. Recent rapid progress of the computational chemistry enables us to study potential energy surfaces in detail by means of ab initio quantum chemical calculation. For example, stable structures and potential energy surfaces of the N_2O_2 system have been already reported.[19] For the $N_2O_2^+$ system, however, a detailed reaction mechanism has not been discussed because there has been no information about structures of the $N_2O_2^+$ reaction intermediate complexes and related potential energy surfaces in terms of quantum chemical approach as far as we are aware, although Janik and Conway discussed the bond energy and entropy change in the ($N_2\cdots O_2^+$) cluster by an empirical potential energy surface.[20] Accordingly in this paper, we carried out ab initio quantum chemical calculations and investigated the reaction mechanism for the $N_2^+ + O_2$ reaction system.

Computational Methods

Ab initio molecular computations reported in this article were performed with Gaussian 94 and MOLPRO program packages.[21,22] We carried out geometry optimizations of the reactants, the reaction intermediate complexes, and the products with the 6-31G* basis sets[23] with the second-order Møller−Plesset full-cored perturbational treatment[24] using the Gaussian 94 program.[21] The spin-unrestricted formalism (UMP2) and the approximate spin-projected (PMP2) calculations were performed for all the species except the singlet state. Analytical vibrational frequencies were computed to ensure that each structure corresponds to a true minimum (no negative eigenvalues) at the MP2(full) level. For the optimized UMP2 geometries, energies were calibrated by single and double excitation coupled-cluster (CCSD) calculations, also including a perturbational estimate of connected triple excitations (CCSD(T)).[25] Orbital energies are obtained by the restricted open-shell Hartree−Fock (ROHF) method. In addition, the internally contracted multireference configuration interaction (MRCI) calculations[26] with 6-31G* basis set were performed by the MOLPRO program.[22]

Results and Discussions

Figure 1 shows the electronic state correlation diagram of the $N_2^+ + O_2$ reaction system at the CCSD(T)/6-31G*//UMP2-(full)/6-31G* level with zero-point energy (ZPE) correction at the MP2(full)/6-31G* level factored by 0.94. Our calculation also shows that the ground state of N_2^+ is $^2\Sigma_g^+$, and then the energies of the other states are measured relative to the N_2^+-($^2\Sigma_g^+$) + $O_2(^3\Sigma_g^-)$ state. The MRCI calculations for the reactants ($N_2^+(^2\Sigma_g^+)$, $N_2^+(^2\Pi_u)$, and $O_2(^3\Sigma_g^-)$) and the products (O_2^+-($^2\Pi_g$), $O_2^+(^4\Pi_u)$, and $N_2(^1\Sigma_g^+)$) of the CT reaction were carried out by considering $2\sigma_g$, $2\sigma_u$, $3\sigma_g$, $1\pi_u$, $1\pi_g$, and $3\sigma_u$ orbitals as the active space, with geometry optimization. For CT reaction 1, the calculated energies both by CCSD(T) and by MRCI are consistent with the experimental data. For the abstraction reactions, the PMP2(full) calculations are more consistent with the experimental results than with the CCSD(T) results when the product system consists of only the monatomic and diatomic species as in the reactions 4 and 5. However, for the reaction 3 where $N_2O^+(^2\Pi)$ is produced, the CCSD(T) results are more consistent with the experimental data. The CCSD(T) calculations are more reliable than the PMP2(full) results for polyatomic complexes such as $N_2O_2^+$ intermediate complexes.

Table 1 shows the optimized bond lengths and the vibrational frequencies of the reactants and the products of the CT reaction.

TABLE 1: Optimized Bond Lengths and Vibrational Frequencies of Reactants and Products

species	term	MP2(full)/6-31G* bond length[a]	MP2(full)/6-31G* frequency[b]	MRCI/6-31G* bond length[a]
reactant				
N_2^+	$^2\Sigma_g^+$	1.146	1967	1.140
N_2^+	$^2\Pi_u$	1.203	1649	1.196
O_2	$^3\Sigma_g^-$	1.246	1328	1.232
product				
O_2^+	$^2\Pi_g$	1.187	1269	1.146
O_2^+	$^4\Pi_u$	1.409	898	1.419
N_2	$^1\Sigma_g^+$	1.130	2049	1.121

[a] In units of angstroms. [b] In units of cm^{-1} and scaled by 0.94.

The bond length and frequency of $N_2^+(^2\Sigma_g^+)$ are nearly equal to those of $N_2(^1\Sigma_g^+)$, respectively, and therefore, it is confirmed that the $N_2^+(^2\Sigma_g^+) \rightarrow N_2(^1\Sigma_g^+)$ transition is vertical. In other cases, the bond length and frequency of reactants make some change before and after the CT.

T-Shaped Complexes. The electronic configurations of the reactant system and the CT product system in the ground and excited states are shown in Figure 2. From the viewpoint of the MO in-phase overlapping for the T-shaped complex suggested by Ferguson et al.,[3] in the CT process from $N_2^+(^2\Sigma_g^+)$ an electron is transferred from the $1\pi_u$ orbital of $O_2(^3\Sigma_g^-)$ to the $3\sigma_g$ orbital of $N_2^+(^2\Sigma_g^+)$ with conservation of the spin symmetry in Figure 2a, and then $O_2^+(^4\Pi_u)$ is produced. In this CT process, we found a stable intermediate complex **1**. As Ferguson et al. suggested,[3,6] the geometry of **1** looks like the character "T" with the O_2 fragment forming the top of the T, as shown in Figure 3. The electronic state of **1** is $^4B_1$. The optimized geometrical parameters and Mulliken atomic charges are listed in Table 2. At the CCSD(T) level, the energy of **1** relative to the reactant state is -0.726 eV, and therefore, complex **1** is more stable than the $N_2^+(^2\Sigma_g^+) + O_2(^3\Sigma_g^-)$ reactant system. In complex **1**, the positive charge has already been distributed on the O_2 fragments, where the electronic configuration of **1** is the same as that of the $N_2(^1\Sigma_g^+) + O_2^+(^4\Pi_u)$ product system shown in Figure 2d. It is observed that the $8a_1$ orbital with β-spin electron, which is mainly formed by the $3\sigma_g$ orbital of N_2 fragment, slightly consists of the $1\pi_u$ orbital of the O_2 fragment by coupling the $3\sigma_g$ orbital with the in-phase overlap. According to the vibrational frequency analysis shown in Table 3, the O−O and N−N stretching modes have a large wavenumber, 1023 and 3784 cm^{-1}, respectively, and only one of the bending modes also has a large wavenumber, 1723 cm^{-1}.

Furthermore, we found the most stable intermediate complex **2** of the CT reaction system, whose geometry is also T-shaped with the electronic state $^2A_2$. As shown in Table 2, the distance between N_2 and O_2 fragments is longer than that of **1**, and the O−O and N−N bond lengths are nearly equal to the bond lengths of $O_2^+(^2\Pi_g)$ and $N_2(^1\Sigma_g^+)$ listed in Table 1, respectively. In complex **2**, similarly as in the complex **1**, the positive charge has already been distributed on the O_2 fragments, where the electronic configuration of **2** is the same as that of the $N_2(^1\Sigma_g^+) + O_2^+(^2\Pi_g)$ ground state shown in Figure 2c. Complex **2** has been discussed by experimentalists as the $(N_2\cdots O_2^+(X))$ complex[4,6] that would immediately dissociate to $N_2(^1\Sigma_g^+) + O_2^+(^2\Pi_g)$ because of the large exothermicity. As shown in Table 3, the O−O and N−N stretching modes respectively have a large wavenumber, 1276 and 2059 cm^{-1} and their values are close to the frequencies of the corresponding compounds of the product, $O_2^+(^2\Pi_g)$ and $N_2(^1\Sigma_g^+)$, listed in Table 1. By contrast, wavenumbers of the other four vibrational modes range over 117−313 cm^{-1}, and thus, the weakness of the bonding between N_2 and O_2 fragments is confirmed.[6]

Analysis of the $N_2^+(^2\Sigma_g^+;v) + O_2$ Reactions Observed by Kato et al. We have studied a model of the CT process in which the $N_2O_2^+$ system is assumed to have the shape of a T during the reaction. Then the symmetry C_{2v} is kept in this model. The geometry of the system is characterized by three parameters, r_1, r_2, and r_3, which are defined in Figure 3; r_1 and r_3 are the lengths of the N−N and O−O bonds, respectively. The rest parameter r_2 is the distance between the N_2 and O_2 fragments. We fixed r_1 and r_3 at the optimized values for the reactants or the products, which are given in Table 1. We then calculated the potential energy of the $N_2O_2^+$ system as a function of r_2. The potential energy of the $N_2O_2^+$ T-shaped model has been determined by means of the MRCI calculations, where 21 electrons and 14 orbitals were considered as the active space.

The plots of the potential energies with respect to r_2 at the MRCI level are shown in Figure 4. Along the reaction path with the quartet state before reaching complex **1**, our calculation shows that the electronic configuration is dominated by the quartet $N_2^+(^2\Sigma_g^+) + O_2(^3\Sigma_g^-)$ reactant system, which is shown in Figure 2a, and the potential energy profile is drawn in the left half of Figure 4. We have confirmed that the potential energy curve is completely flat in the initial stage of this reaction path, and then it gradually decreases where the distance r_2 shrinks to be shorter than 4 Å; that is, there is no barrier along the potential curve from the reactant system to complex **1** when the space symmetry C_{2v} is kept. When r_2 is shortened, the reference coefficient in the MRCI calculations for the configuration of the $N_2(^1\Sigma_g^+) + O_2^+(^4\Pi_u)$ CT product system is enhanced. For the succeeding reaction path starting from the complex **1**, the electronic configuration smoothly converges to the product system and the potential energies are plotted in the right half of Figure 4. The potential energy curve rises monotonically as the distance r_2 is lengthened starting from **1**. It is supposed that the $N_2(^1\Sigma_g^+) + O_2^+(^4\Pi_u)$ product system is not always obtained after the complex **1** is formed because the energy of the $N_2(^1\Sigma_g^+) + O_2^+(^4\Pi_u)$ product system is higher by ca. 1.0 eV than that of the complex **1**. The impulsive collision in the repulsive part of the potential well due to complex **1** would pull back the $N_2O_2^+$ system to **1**, or it would return the CT again to the O_2 fragment to reproduce the reactant system. This is because the potential energy of the reactant system is lower than that of the product system if $r_2 > 2.5$ Å, and hence, the reactant system $N_2^+(^2\Sigma_g^+) + O_2(^3\Sigma_g^-)$ can be recovered with vibrational deactivation by short-range intermolecular vibrational energy transfer and not by the long-range classical Landau−Teller mechanism.[27]

In the left of Figure 4 the plot of the potential energies along the reaction path from the doublet reactant system $N_2^+(^2\Pi_u) + O_2(^3\Sigma_g^-)$ to complex **2** is also shown. Here, we fixed r_1 at the optimized values for $N_2^+(^2\Sigma_g^+)$ in order to compare the energy of the doublet surface with that of the quartet surface at the same geometry. We found that the energy increases as the N_2 and O_2 fragments separate from complex **2** to the doublet reactant system. It was also observed that as they are separated farther, the reference coefficient to the $N_2^+(^2\Pi_u) + O_2(^3\Sigma_g^-)$ state contributed more to the MRCI calculation. But the energy is much lower than that of the $N_2^+(^2\Sigma_g^+) + O_2(^3\Sigma_g^-)$ reactant system and did not exceed it when their distance r_2 reaches 8 Å because the $N_2(^1\Sigma_g^+) + O_2^+(^2\Pi_g)$ reference state, which is an extremely stable state, has a large effect in reducing the energy of the doublet reactant system with C_{2v} symmetry. This means that the energy surface of the doublet $N_2^+(^2\Pi_u) + O_2(^3\Sigma_g^-)$ state does not cross that of the quartet $N_2^+(^2\Sigma_g^+) + O_2(^3\Sigma_g^-)$ state when the space symmetry C_{2v} is kept. Even if

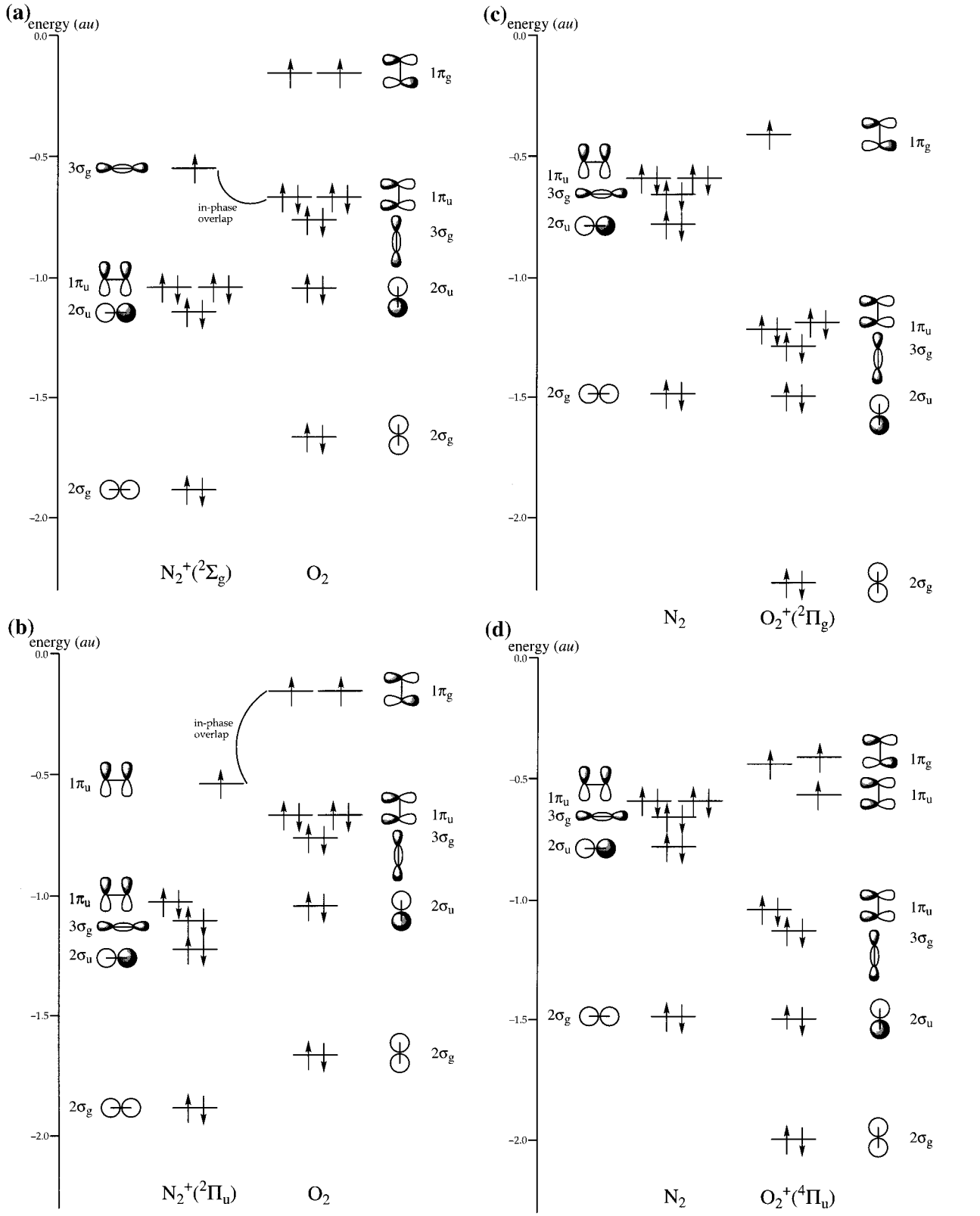

Figure 2. Electronic configurations at the ROHF/6-31G* level for (a) the ground state and (b) the excited state of reactant system and for (c) the ground state and (d) the excited state of product system in the charge-transfer reaction.

the doublet and quartet surfaces cross with the C_{2v} symmetry, the electron transition from the quartet surface to the doublet surface is symmetry-forbidden. Therefore, for the $N_2^+(^2\Sigma_g^+) + O_2(^3\Sigma_g^-)$ reaction system, the short-range intermediate complex mechanism along the quartet surface would be conserved with the shape of a T during the reaction, and the system floats near complex **1** without the electron transition to the doublet surface when the space symmetry C_{2v} is kept.

The reaction path from complex **2** to the $N_2(^1\Sigma_g^+) + O_2^+(^2\Pi_g)$ CT product system in the doublet state is almost flat as shown in the right of Figure 4. Moreover, complex **2** possesses almost the same vibrational characteristics as that of the N_2-

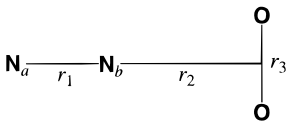

1 and **2**

Figure 3. T-shaped complexes **1** and **2**.

TABLE 2: Optimized Geometrical Parameters and Mulliken Atomic Charges for the T-Shaped $N_2O_2^+$ Complexes at the UMP2/6-31G* Level[a]

		geometrical parameters[b]			Mulliken atomic charges		
	term	r_1	r_2	r_3	N_a	N_b	O
1	$^4B_1$	1.094	2.012	1.332	+0.145	+0.065	+0.395
2	$^2A_2$	1.129	2.732	1.186	+0.098	−0.089	+0.495

[a] Refer to Figure 3 for subscripts of *r* and nitrogen atoms. [b] In units of angstroms.

TABLE 3: Frequencies of Vibrational Modes of the T-Shaped $N_2O_2^+$ Complexes at the UMP2/6-31G* Level[a]

	stretching modes		
	ν(N−N)	ν(O−O)	bending modes
1	3784 (a_1)	1023 (a_1)	1723 (b_2), 318 (a_1), 18 (b_1), 8 (b_2)
2	2059 (a_1)	1276 (a_1)	313 (b_2), 141 (a_1), 127 (b_1), 117 (b_2)

[a] In units of cm^{-1} and scaled by 0.94.

($^1\Sigma_g^+$) + $O_2^+(^2\Pi_g)$ product system. Therefore, once the doublet complex **2** is formed, it dissociates directly to the $N_2(^1\Sigma_g^+)$ + $O_2^+(^2\Pi_g)$ product system.

In CT reaction 1 for the $N_2^+(X^2\Sigma_g^+;v)$ + $O_2(X^3\Sigma_g^-)$ system, the electron transfer from the $1\pi_u$ orbital of $O_2(^3\Sigma_g^-)$, whose removal leads to $O_2^+(^4\Pi_u)$, to the $3\sigma_g$ orbital of $N_2^+(^2\Sigma_g^+)$ would be easy to proceed along the potential energy curve with the C_{2v} symmetry in Figure 4 through the concerted reaction pathway due to the in-phase overlap as shown in Figure 2a. However, the dissociation to the $N_2(^1\Sigma_g^+)$ + $O_2^+(^4\Pi_u)$ products is difficult because of the endothermicity for the low vibrational states with $v < 2$, in particular in the case of low E_{CM}. When $v = 2$, CT reaction 1 for the $N_2^+(^2\Sigma_g^+;v)$ + $O_2(^3\Sigma_g^-)$ system to the $N_2(^1\Sigma_g^+)$ + $O_2^+(^4\Pi_u)$ products is exothermic by 0.012 eV, and therefore, it would be possible to reach the $O_2^+(^4\Pi_u)$ state if $v \geq 2$ at some E_{CM} and the CT is expected to be enhanced to some extent.[7]

On the other hand, the electron transfer from the $1\pi_g$ orbital of $O_2(^3\Sigma_g^-)$, whose removal leads to $O_2^+(^2\Pi_g)$, to the $3\sigma_g$ orbital of $N_2^+(^2\Sigma_g^+)$ is symmetry-forbidden in MO overlapping for the rectangular T-shaped complex as shown in Figure 2a. Despite the high exothermicity of the CT, there is no probability of the electron transfer to produce $O_2^+(^2\Pi_g)$ from the $N_2^+(^2\Sigma_g^+)$ + $O_2(^3\Sigma_g^-)$ reactant system along the C_{2v} potential energy curve. For the formation of $O_2^+(^2\Pi_g)$ from the $N_2^+(^2\Sigma_g^+)$ + $O_2(^3\Sigma_g^-)$ reactant system, a break of the C_{2v} symmetry is hereby necessary. An in-phase MO overlap between N_2 and O_2 fragments can be produced when the C_{2v} symmetry is broken, and then the formation of $O_2^+(^2\Pi_g)$ by means of the CT from $O_2(^3\Sigma_g^-)$ to $N_2^+(^2\Sigma_g^+)$ would occur.

The fact that the rate constant of the CT, k_{CT}, is much smaller than that of vibrational deactivation of $N_2^+(^2\Sigma_g^+;v)$, k_q, can be explained by the difference in the geometrical symmetry of the system. Namely, the $N_2^+(^2\Sigma_g^+;v)$ + $O_2(^3\Sigma_g^-)$ system mostly would form complex **1** smoothly along the quartet surface with C_{2v} symmetry because the C_{2v} geometry is more stable than the distorted T-shape geometry around the reaction path. As above-mentioned, the short-range intermediate complex mechanism along the quartet surface with C_{2v} symmetry would be conserved without the transition to the doublet surface once complex **1** is formed and then dissociate back to the reactant system for the low vibrational energy state with the vibrational deactivation along the quartet surface. On the other hand, the CT to produce $O_2^+(^2\Pi_g)$ from the $N_2^+(^2\Sigma_g^+)$ + $O_2(^3\Sigma_g^-)$ reactant system cannot occur when space symmetry C_{2v} is kept. The distortion of the C_{2v} geometry in order to produce $O_2^+(^2\Pi_g)$ would be at a disadvantage because the distorted geometry has a higher energy than the C_{2v} geometry and it is expected that the in-phase MO overlap between N_2 and O_2 fragments for the distorted system is not so large.

Analysis of the $N_2^+(^2\Sigma_g^+,^2\Pi_u;v)$ + O_2 Reactions Observed by Koyano et al. In CT reaction 1, Koyano et al. observed that the CT cross section for the $N_2^+(^2\Pi_u)$ + $O_2(^3\Sigma_g^-)$ reactant system is larger by far than that for the $N_2^+(^2\Sigma_g^+)$ + $O_2(^3\Sigma_g^-)$ reactant system by experiments with large translational energy.[2] CT reaction 1 from $N_2^+(^2\Sigma_g^+)$ + $O_2(^3\Sigma_g^-)$ to $N_2(^1\Sigma_g^+)$ + O_2^+-($^2\Pi_g$) would proceed with distortion of the C_{2v} geometry so that the cross section of the CT is very small despite the high exothermicity. For the $N_2^+(^2\Pi_u)$ + $O_2(^3\Sigma_g^-)$ reactant system, in contrast with the case of $N_2^+(^2\Sigma_g^+)$, the electron transfer from the $1\pi_g$ orbital of $O_2(^3\Sigma_g^-)$ to the SOMO, namely, the $1\pi_u$ orbital of $N_2^+(^2\Pi_u)$, is easy because their in-plane MO overlapping in the T-shaped complex with C_{2v} symmetry is in phase. The large cross sections of the CT for $N_2^+(^2\Pi_u)$ can be explained by the in-phase overlap with high exothermicity in the CT reaction.

For the doublet state, we found stable $N_2O_2^+$ complexes with bent structure. Table 4 lists the optimized geometrical parameters and Mulliken atomic charges of bent $N_2O_2^+$ complexes **3** ($^2A''$) and **4** ($^2A'$). Charge distribution on the bent complexes **3** and **4** is in striking contrast to the distribution on the complex **2**; that is, positive charge is distributed exclusively on the N_2 fragment of complexes **3** and **4**. Both of the bent complexes clearly have an occupied N−N σ bonding MO of β-spin electron, which mainly consists of 2p orbitals of each nitrogen atom like the $3\sigma_g$ orbital of the $N_2^+(^2\Pi_u)$ ion, and accordingly, it is considered that the reactant state that leads to these complexes is $N_2^+(^2\Pi_u)$ + $O_2(^3\Sigma_g^-)$ rather than $N_2^+(^2\Sigma_g^+)$ + $O_2(^3\Sigma_g^-)$ because the N−N σ bonding MO of the β-spin like the $3\sigma_g$ orbital of N_2^+ corresponds to an occupied MO for $N_2^+(^2\Pi_u)$ and an unoccupied MO for $N_2^+(^2\Sigma_g^+)$. One $1\pi_g$ electron of $O_2(^3\Sigma_g^-)$ is left on the terminal oxygen atom of the bent complexes, and the other $1\pi_g$ electron interacts with the SOMO of $N_2^+(^2\Pi_u)$ on the N−N−O part. The interaction scheme is in a like the antiferromagnetic one between localized spins. The electronic state of bent complexes is $^2A''$ (**3**) when the orbital interaction is in-plane, while it is $^2A'$ (**4**) when the orbital interaction is out-of-plane with respect to the $N_2O_2^+$ plane. Almost all of spin density is located on the terminal oxygen atom for both of the bent complexes. For complex **3**, the O−O and N−N stretching modes have a large wavenumber, 1042 and 2205 cm^{-1}, respectively, while wavenumbers of the other four vibrational modes are 195−652 cm^{-1}, and thus, it is found that the bonding between N_2 and O_2 fragments is relatively weak. For complex **4**, the O−O and N−N stretching modes have a large wavenumber, 1588 and 3476 cm^{-1}, respectively, while wavenumbers of the other four vibrational modes are 110−1055 cm^{-1} so that the characteristics similar to those of complex **3** are recognized with respect to the bonding between N_2 and O_2 fragments.

In particular, complex **3** has a large stabilization energy by ca. 2 eV relative to the $N_2^+(^2\Pi_u)$ + $O_2(^3\Sigma_g^-)$ reactant system at the CCSD(T) level. The doublet complexes **2** and **3** are

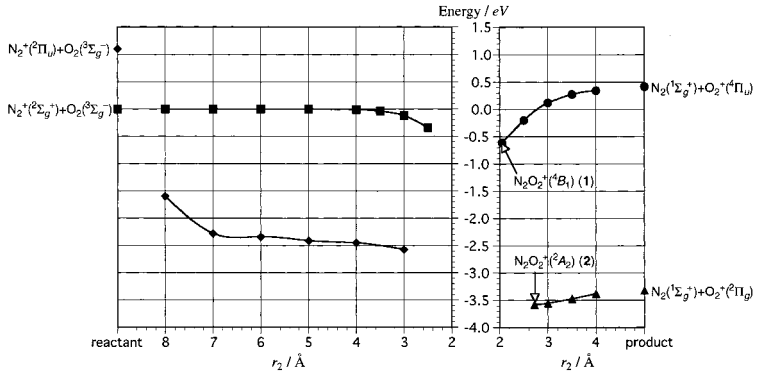

Figure 4. Potential energy curves for the C_{2v} charge-transfer reaction pathways at the MRCI/6-31G* level. The symbols "■", "◆", "●" and "▲" respectively denote the $N_2^+(^2\Sigma_g^+) + O_2(^3\Sigma_g^-)$ reactant state, the $N_2^+(^2\Pi_u) + O_2(^3\Sigma_g^-)$ reactant state, the $N_2(^1\Sigma_g^+) + O_2^+(^4\Pi_u)$ product state, and the $N_2(^1\Sigma_g^+) + O_2^+(^2\Pi_g)$ product state. Refer to Figure 3 for the geometry.

TABLE 4: Optimized Geometrical Parameters and Mulliken Atomic Charges for the Bent $N_2O_2^+$ Complexes at the UMP2/6-31G* Level[a]

		geometrical parameters[b]			
	term	$r(N_a-N_b)$	$r(N_b-O_a)$	$r(O_a-O_b)$	$r(N_a-O_b)$
3	$^2A''$	1.139	1.358	1.355	
4	$^2A'$	1.159	1.285	1.432	
5	$^4A'$	1.096	1.240	2.952	3.079

	geometrical parameters[b]		Mulliken atomic charges			
	$\theta(N_a-N_b-O_a)$	$\theta(N_b-O_a-O_b)$	N_a	N_b	O_a	O_b
3	176.0	108.6	+0.334	+0.544	−0.089	+0.211
4	175.0	105.8	+0.342	+0.581	−0.166	+0.242
5	178.8	69.6	+0.308	+0.705	−0.025	+0.013

[a] Refer to Figure 5 for subscripts of atoms. The dihedral angle $\phi(N_a-N_b-O_a-O_b)$ is 180° for all of the bent $N_2O_2^+$ complexes. [b] Bond length r is in units of angstroms, and bond angle θ is in degrees.

located on the same potential energy surface, which has an out-of-plane unpaired electron with respect to the $N_2O_2^+$ plane, and the barrier between **2** and **3** is expected to be small, judging from the results of vibrational analysis. Therefore, the formation of complex **2** or $O_2^+(^2\Pi_g)$ from the $N_2^+(^2\Pi_u) + O_2(^3\Sigma_g^-)$ reactant system can occur not only along the C_{2v} reaction path but also via complex **3** along the path of the $^2A''$ state with bent geometry and an out-of-plane unpaired electron with respect to the $N_2O_2^+$ plane. Moreover, the formation of $O_2^+(^2\Pi_g)$ from the $N_2^+(^2\Pi_u) + O_2(^3\Sigma_g^-)$ reactant system can also occur via complex **4** along the path of the $^2A'$ state with bent geometry and an in-plane unpaired electron with respect to the $N_2O_2^+$ plane, similar to the path of the $^2A''$ state. In addition, it is expected that the energy surfaces of these doublet states with the bent geometry would respectively cross that of the quartet state with the distorted geometry to produce $O_2^+(^2\Pi_g)$ from the $N_2^+(^2\Sigma_g^+) + O_2(^3\Sigma_g^-)$ reactant system when the space symmetry C_{2v} is broken.

Analysis of the $N_2^+(^2\Sigma_g^+) + O_2$ Reactions Observed by Schultz and Armentrout. The CT reaction 1 for the $N_2^+(^2\Sigma_g^+) + O_2(^3\Sigma_g^-)$ reactant system has been discussed in this article in terms of the short-range intermediate complex mechanism. The experimental results by Schultz and Armentrout for $E_{CM} \geq 1$ eV can be explained by this mechanism. For the abstraction reactions 3−5, the bent $N_2O_2^+$ complex **5** with the quartet state, $^4A'$, plays an important role. Complex **5** is an excited state of the quartet $N_2O_2^+$ complex **1**, and one of the oxygen atoms is separated from the remaining N−N−O part as shown in Table 4. Similar to complexes **3** and **4**, the positive charge is distributed on the N_2 fragment of **5**. Two unpaired electrons of the reactant $O_2(^3\Sigma_g^-)$ are left on the separated oxygen atom in **5** as an in-plane and an out-of-plane unpaired electron with respect to the $N_2O_2^+$ plane. The other unpaired electron of **5** occupies an out-of-plane π orbital, which has lobes on the edges of the N−N−O part, like the SOMO of the allyl radical. This out-of-plane π orbital originates from the SOMO of the reactant $N_2^+(^2\Pi_u)$ on condition that the orientation of the SOMO is vertical to the $N_2O_2^+$ plane. To form complex **5** from the ground state of the reactant system, $N_2^+(^2\Sigma_g^+) + O_2(^3\Sigma_g^-)$, it is necessary to make the surface crossing to the surface, which leads to the $N_2^+(^2\Pi_u) + O_2(^3\Sigma_g^-)$ reactant system, similar to the formation of complex **2** from the $N_2^+(^2\Sigma_g^+) + O_2(^3\Sigma_g^-)$ system.

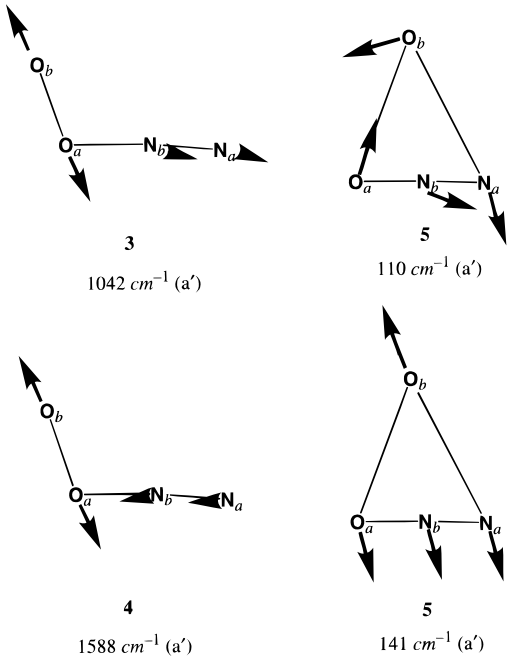

Figure 5. Eigenvectors of the O−O stretching mode of the doublet bent complexes **3** and **4** and the quartet bent complex **5** at the UMP2-(full)/6-31G* level.

Complex **5** is characterized by the very long O−O and N−O bonds, and accordingly, it is expected that these bonds are extremely weak. According to the vibrational frequency analysis shown in Figure 5, the vibrational modes related to O−O and N−O stretching of **5** have very small wavenumbers, 110 and 141 cm^{-1}, which are respectively ca. 0.11−0.14 and 0.07−0.09 times as large as the O−O stretching vibrational wavenumber of the doublet bent complexes **3** and **4** and smaller than the bending vibrational wavenumber of the quartet T-shaped complex **1** in Table 3. The behavior of the lowest vibrational mode implies that the N_2 and O_2 fragments are weakly attached

TABLE 5: Optimized Geometrical Parameters and Mulliken Atomic Charges for N_2O^+ and NO^+ Products at the UMP2/6-31G* Level[a]

			geometrical parameters[a]			Mulliken atomic charges		
		term	r(N−N)	r(N−O)	θ(NNO)	N (edge)	N (mid)	O
N_2O^+	**6**	$^2\Pi$	1.097	1.242	180.0	+0.326	+0.697	−0.023
	7	$^4A''$	2.967	1.092	113.1	+0.010	+0.750	+0.240
	8	$^4\Sigma^-$	1.107	2.254	180.0	+0.130	−0.052	+0.922
NO^+	**9**	$^1\Sigma^+$		1.102		+0.621		+0.379

[a] Bond length r is in units of angstroms, and bond angle θ is in degrees.

TABLE 6: Frequencies of Stretching Modes of N_2O^+ Compounds at the UMP2/6-31G* Level[a]

	ν(N−N)	ν(N−O)
6	3082	902
7	98	4099
8	3564	221

[a] In units of cm^{-1} and scaled by 0.94.

to form complex **5**, and that of the second lowest vibrational mode indicates that the cleavage into an O atom and an N_2O molecule is easy in the quartet bent complex **5**. Therefore, this complex should largely contribute to abstraction reaction 3. Actually, the electronic states of the N−N−O part and the separated oxygen atom are nearly equal to those of $N_2O^+(^2\Pi)$ and O (^{3}P), respectively.

Table 5 shows the optimized geometrical parameters of N_2O^+ and NO^+ ions, which are the products of abstraction reactions 3−5 reported by Schultz and Armentrout.[4] The ground state of the N_2O^+ ion **6** ($^2\Pi$) has a linear structure with doublet spin state. This ion is easy to obtain without a change of the electronic structure once complex **5** is formed. The excited states of the N_2O^+ ion in quartet states, **7**($^4A''$) and **8**($^4\Sigma^-$), are more unstable by 0.535 and 0.870 eV, respectively, than the ground state **6** at the CCSD(T) level.

The optimized geometry of **7**, $N_2O^+(^4A'')$, is a bent structure and characterized by a very long N−N bond, and accordingly, it is expected that the N−N bond is very weak. As listed in Table 6, the N−N stretching mode has a very small wavenumber, 98 cm^{-1}, while the N−O stretching mode has very large wavenumber, 4099 cm^{-1}. All of the unpaired electrons are located on the separated N atom, and the electronic structures of the N−O part and the separated N atom are identical to those of $NO^+(^1\Sigma^+)$ (**9**) and N(^{4}S), respectively. Therefore, it is confirmed that the N−N bond of $N_2O^+(^4A'')$ is easy to cleave and that $NO^+(^1\Sigma^+)$ and *N*(^{4}*S*), the products of reaction 4, are obtained.[4,17]

On the other hand, the optimized geometry of **8**, $N_2O^+(^4\Sigma^-)$, has a linear structure and characterized by a very long N−O bond, and accordingly, it is expected that the N−O bond is very weak. The N−N stretching mode has very large wavenumber, 3564 cm^{-1}, while the N−O stretching mode has very small wavenumber, 221 cm^{-1}. Here, all of the unpaired electrons are located on the separated O atom, and the electronic structures of the N−N part and the separated O atom are identical to those of $N_2(^1\Sigma_g^+)$ and $O^+(^4S)$, respectively. Therefore, it is confirmed that the N−O bond of $N_2O^+(^4\Sigma^-)$ is easy to cleave, and $N_2(^1\Sigma_g^+)$ and $O^+(^4S)$, the products of reaction 5, are obtained.[4,17]

These excited N_2O^+ ions **7** and **8** should be situated on the same potential energy surface with an energy barrier separating **7** from **8**.[17,18] This surface is different from the surface which contains the complex **5** and the ground state of N_2O^+ ion **6**, and therefore the excited N_2O^+ ions **7** and **8** cannot be directly obtained from the complex **5**.

For the N_2O^+ ion **6**, both of the N−O and N−N stretching modes of $N_2O^+(^2\Pi)$ have large wavenumber, 902 and 3082 cm^{-1}, respectively, and therefore, both of the N−O and N−N bonds are strong. If the cleavage into NO^+ and N takes place like $N_2O^+(^4A'')$, the electronic states of the products are $NO^+(^1\Sigma^+)$ (**9**) and N(^{2}*D*),[4,17] where the heat of reaction is extremely endothermic as shown in Figure 1. It is considered that the direct cleavage into **9** and N(^{2}*D*) is hard to occur at low E_{CM} once $N_2O^+(^2\Pi)$ is formed. It has been reported that the $NO^+(^1\Sigma^+)$ + N(^{4}S) system and the $O^+(^4S)$ + $N_2(^1\Sigma_g^+)$ system can lead to the ground state of $N_2O^+(^2\Pi)$ by means of the surface crossing with large exothermicity.[17]

According to the experimental results by Schultz and Armentrout, the cross section for formation of NO^+ rises slowly from a threshold of ∼2 eV and then much more rapidly above ca. 4.5 eV with respect to the collisional energy.[4] The reason the cross section to product NO^+ is small at low E_{CM} can be explained by the surface crossing from $N_2O^+(^2\Pi)$ to $NO^+(^1\Sigma^+)$ + N(^{4}S). At high E_{CM}, above 4.5 eV, NO^+ can be formed efficiently along the potential energy surface with $C_{\infty v}$ symmetry from $N_2O^+(^2\Pi)$ to $NO^+(^1\Sigma^+)$ + N(^{2}D). For formation of O^+, the cross section rises at a threshold of 3 eV accompanying reduction of the cross section for N_2O^+.[4] It means that O^+ is obtained from $N_2O^+(^2\Pi)$ to $O^+(^4S)$ + $N_2(^1\Sigma_g^+)$ by the surface crossing similarly as the formation of NO^+ at low E_{CM}.

Conclusions

In this article, we have investigated the reaction mechanism of the $N_2^+ + O_2$ reaction system and discussed related matters. For the charge-transfer reaction, reactivity and collision energy dependence are characteristic of the electronic and vibrational state of N_2^+.[2,4,6,7] It is caused by the difference in mechanism of electron transfer. Electron transfer to $N_2^+(A^2\Pi_u)$ occurs via a doublet T-shaped intermediate complex $N_2O_2^+(^2A_2)$ with in-phase MO overlap between the $1\pi_g$ orbital of $O_2(X^3\Sigma_g^-)$ and $1\pi_u$ orbital of $N_2^+(A^2\Pi_u)$ when the space symmetry C_{2v} is kept. The interaction between N_2 and O_2 fragments is extremely weak in the $N_2O_2^+(^2A_2)$ complex so that the potential energy surface around the $N_2O_2^+(^2A_2)$ complex is very flat. The electronic states of the N_2 and O_2 fragments of the $N_2O_2^+(^2A_2)$ complex are respectively equal to those of $N_2(X^1\Sigma_g^+)$ and $O_2^+(X^2\Pi_g)$, and this complex would immediately dissociate to $N_2(X^1\Sigma_g^+) + O_2^+(X^2\Pi_g)$.

On the other hand, electron transfer to $N_2^+(X^2\Sigma_g^+)$ occurs by a short-range mechanism via a quartet T-shaped intermediate complex $N_2O_2^+(^4B_1)$, which is located at the vivid minimum of the potential energy surface when the space symmetry C_{2v} is kept. In the $N_2O_2^+(^4B_1)$ complex, positive charge has already been distributed on the O_2 fragment just like in the $N_2(X^1\Sigma_g^+) + O_2^+(a^4\Pi_u)$ system. We have confirmed that there is no barrier from the reactants to the $N_2O_2^+(^4B_1)$ complex. The $N_2O_2^+(^4B_1)$ complex also works as a deep potential well for the vibrational deactivation of $N_2^+(X^2\Sigma_g^+;v)$.[6,7] For the state of low energy, the impulsive collision in the repulsive part of the potential well would pull back the $N_2O_2^+$ system to the $N_2O_2^+(^4B_1)$ complex; otherwise, it would give rise to the CT again to the reactant with vibrational deactivation by intermolecular vibrational energy transfer. The enhancement of the CT reaction for $v \geq 2$ and vibrational deactivation of the $N_2^+(X^2\Sigma_g^+) + O_2$ reactant system can be successfully explained in terms of the short-range intermediate complex mechanism. Once the $N_2O_2^+(^4B_1)$ complex is formed, it would be conserved along the reaction path by the short-range intermediate complex mechanism on a quartet surface with the C_{2v} symmetry without the transition to the

doublet surface. The $O_2^+(X^2\Pi_g)$ product from the $N_2^+(X^2\Sigma_g^+) + O_2$ reactant system cannot be obtained when the space symmetry C_{2v} is kept, namely, the $O_2^+(X^2\Pi_g)$ product by CT to $N_2^+(X^2\Sigma_g^+)$ should be obtained when the space symmetry C_{2v} is broken.

The bent complexes with the doublet state, $N_2O_2^+(^2A'')$ and $N_2O_2^+(^2A')$, have O−O and N−N stretching modes with large wavenumber, and positive charge is distributed on the N_2 fragment in these complexes. These complexes are halfway on the reaction paths of the CT to produce $O_2^+(X^2\Pi_g)$ from the $N_2^+(A^2\Pi_u) + O_2$ reactant system with bent N_2O_2 geometry.

The bent complex in the quartet state $N_2O_2^+(^4A')$ has very long O−O and N−O bonds; that is, one oxygen atom is separated from the N−N−O part. The electronic states of the N−N−O part and the separated oxygen atom are nearly equal to those of $N_2O^+(^2\Pi)$ and $O(^3P)$, respectively. Both of the O−O and N−O stretching vibrations with long bond lengths have very small wavenumbers, and these bonds are easy to cleave. Therefore, $N_2O_2^+(^4A')$ largely contributes to the abstraction reaction forming the ground state of $N_2O^+(^2\Pi)$. The excited states of $N_2O^+(^4A'',^4\Sigma^-)$ are not directly obtained from $N_2O_2^+(^4A')$. The formation of $NO^+(^1\Sigma^+) + N(^4S)$ and $O^+(^4S) + N_2(^1\Sigma_g^+)$ from $N_2O^+(^2\Pi)$ occurs by means of surface crossing.

Acknowledgment. This work was supported by a Grant-in-Aid for Scientific Research from the Ministry of Education, Science and Culture of Japan, for which the authors express their gratitude. We thank the Computer Center of Institute for Molecular Science and Data Processing Center of Kyoto University for their generous permission to allow us to use the HITAC M-680 and S-820, and FACOM M-780/30, VP-400E, and VP-200 computers, respectively. A.T. thanks Dr. Shuji Kato for sending him ref 7 prior to publication and for a critical reading of this manuscript. K.N. is a research fellow of the Japan Society for the Promotion of Science.

References and Notes

(1) (a) Sheridan, J. R.; Merlo, T.; Enzweiler, J. A. *J. Geophys. Res. A* **1979**, *84*, 7302. (b) Ferguson, E. E.; Fehsenfeld, F. C.; Albritton, D. L. In *Gas-Phase Ion Chemistry*; Bowers, M. T., Ed.; Academic: New York, 1979; Vol. 1, p 45. (c) Smith, D.; Adams, N. G. *Top. Curr. Chem.* **1980**, *89*, 1. (d) Abdou, W. A.; Torr, D. G.; Richards, P. G.; Torr, M. R. *J. Geophys. Res. A* **1982**, *87*, 6324. (e) Abdou, W. A.; Torr, D. G.; Richards, P. G.; Torr, M. R.; Breig, E. L. *J. Geophys. Res. A* **1984**, *89*, 9069.

(2) Koyano, I.; Tanaka, K.; Kato, T.; Suzuki, S. *Faraday Discuss. Chem. Soc.* **1987**, *84*, 265.

(3) Ferguson, E. E.; Richter, R.; Lindinger, W. *J. Chem. Phys.* **1988**, *89*, 1445.

(4) Schultz, R. H.; Armentrout, P. B. *J. Chem. Phys.* **1991**, *95*, 121.

(5) (a) McFarland, M.; Albritton, D. L.; Fehsenfeld, F. C.; Ferguson, E. E.; Schmeltekopf, A. L. *J. Chem. Phys.* **1973**, *59*, 6620. (b) Kobayashi, N.; Kaneko, Y. *J. Phys. Soc. Jpn.* **1974**, *37*, 1082.

(6) Kato, S.; Frost, M. J.; Bierbaum, V. M.; Leone, S. R. *Can. J. Chem.* **1994**, *72*, 625.

(7) Kato, S.; Bierbaum, V. M.; Leone, S. R. *J. Phys. Chem. A* **1998**, *102*, 6659.

(8) Dobler, W.; Villinger, H.; Howorka, F.; Lindinger, W. *Int. J. Mass Spectrosc. Ion Phys.* **1983**, *47*, 171.

(9) (a) Lindinger, W.; Fehsenfeld, F. C.; Schmeltekopf, A. L.; Ferguson, E. E. *J. Geophys. Res. A* **1974**, *79*, 4753. (b) Smith, D.; Adams, N. G.; Miller, T. M. *J. Chem. Phys.* **1978**, *69*, 308. (c) Alge, E.; Lindinger, W. *J. Geophys. Res. A* **1981**, *86*, 871. (d) Kemper, P. R.; Bowers, M. T. *J. Chem. Phys.* **1984**, *81*, 2634.

(10) Lindinger, W.; Albritton, D. L.; McFarland, M.; Fehsenfeld, F. C.; Schmeltekopf, A. L.; Ferguson, E. E. *J. Chem. Phys.* **1975**, *62*, 4101.

(11) Laudenslager, J. B.; Huntress, W. T., Jr.; Bowers, M. T. *J. Chem. Phys.* **1974**, *61*, 4600.

(12) (a) Schultz, R. H.; Armentrout, P. B. *Chem. Phys. Lett.* **1991**, *179*, 429. (b) Fisher, E. R.; Armentrout, P. B. *Chem. Phys. Lett.* **1991**, *179*, 435. (c) Schultz, R. H.; Armentrout, P. B. *J. Chem. Phys.* **1992**, *96*, 1036. (d) Weber, M. E.; Dalleska, N. F.; Tjelta, B. L.; Fisher, E. R.; Armentrout, P. B. *J. Chem. Phys.* **1993**, *98*, 7855. (e) Kickel, B. L.; Fisher, E. R.; Armentrout, P. B. *J. Phys. Chem.* **1993**, *97*, 10198. (f) Freysinger, W.; Kahn, F. A.; Armentrout, P. B.; Tosi, P.; Dmitriev, O.; Bassi, D. *J. Chem. Phys.* **1994**, *101*, 3688. (g) Kato, S.; Frost, M. J.; Bierbaum, V. M.; Leone, S. R. *Rev. Sci. Instrum.* **1993**, *64*, 2808. (h) Frost, M. J.; Kato, S.; Bierbaum, V. M.; Leone, S. R. *J. Chem. Phys.* **1994**, *98*, 5993. (i) Frost, M. J.; Kato, S.; Bierbaum, V. M.; Leone, S. R. *J. Chem. Phys.* **1994**, *100*, 6359. (j) Kato, S.; de Gouw, J. A.; Lin, C.-D.; Bierbaum, V. M.; Leone, S. R. *Chem. Phys. Lett.* **1996**, *256*, 305. (k) Kato, S.; de Gouw, J. A.; Lin, C.-D.; Bierbaum, V. M.; Leone, S. R. *J. Chem. Phys.* **1996**, *105*, 5455. (l) Wyttenbach, T.; Bowers, M. T. *J. Phys. Chem.* **1992**, *96*, 8920. (m) Böhringer, H.; Durup-Ferguson, M.; Fahey, D. W.; Fehsenfeld, F. C.; Ferguson, E. E. *J. Chem. Phys.* **1983**, *79*, 4201. (n) Ferguson, E. E. *J. Phys. Chem.* **1986**, *90*, 731. (o) Gislason, E. A.; Ferguson, E. E. *J. Chem. Phys.* **1987**, *87*, 6474. (p) Speller, C. V.; Fitaire, M.; Pointu, A. M. *J. Chem. Phys.* **1983**, *79*, 2190.

(13) Laher, R. R.; Gilmore, F. R. *J. Phys. Chem. Ref. Data* **1991**, *20*, 685.

(14) Gioumousis, G.; Stevenson, D. P. *J. Chem. Phys.* **1958**, *29*, 294.

(15) Fisher, E. R.; Armentrout, P. B. *J. Chem. Phys.* **1990**, *93*, 4858.

(16) Kimura, K.; Katsumata, S.; Achiba, Y.; Yamazaki, T.; Iwata, S. *Handbook of HeI Photoelectron Spectra of Fundamental Organic Compounds*; Halsted: New York, 1981.

(17) Burley, J. D.; Ervin, K. M.; Armentrout, P. B. *J. Chem. Phys.* **1987**, *86*, 1944.

(18) Hopper, D. G. *J. Am. Chem. Soc.* **1978**, *100*, 1019.

(19) (a) Michels, H. H.; Montgomery, J. A., Jr. *J. Chem. Phys.* **1988**, *88*, 7248. (b) Nguyen, K. A.; Gordon, M. S.; Montgomery, J. A., Jr.; Michels, H. H.; Yarkony, D. R. *J. Chem. Phys.* **1993**, *98*, 3845. (c) Nguyen, K. A.; Gordon, M. S.; Montgomery, J. A., Jr.; Michels, H. H. *J. Phys. Chem.* **1994**, *98*, 10072. (d) Nguyen, K. A.; Gordon, M. S.; Boatz, J. A. *J. Am. Chem. Soc.* **1994**, *116*, 9241. (e) Jursic, B. S. *Chem. Phys. Lett.* **1995**, *236*, 206. (f) Jursic, B. S.; Zdravkovski, Z. *Int. J. Quantum Chem.* **1995**, *54*, 161. (g) Chaban, G.; Gordon, M. S.; Nguyen, K. A. *J. Phys. Chem. A* **1997**, *101*, 4283.

(20) Janik, G. S.; Conway, D. C. *J. Phys. Chem.* **1967**, *71*, 823.

(21) Frisch, M. J.; Trucks, G. W.; Schlegel, H. B.; Gill, W. P. M.; Johnson, B. G.; Robb, M. A.; Cheeseman, J. R.; Keith, T. A.; Patterson, G. A.; Montgomery, J. A.; Reghavachari, K.; Al-Laham, M. A.; Zakrzewski, V. G.; Ortiz, J. V.; Foresman, J. B.; Cioslowski, J.; Stefanov, B. B.; Nanayakkara, A.; Challacombe, M.; Peng, C. Y.; Ayala, P. Y.; Chen, W.; Wong, M. W.; Andres, J. L.; Replogle, E. S.; Gomperts, R.; Martin, R. L.; Fox, D. J.; Binkley, J. S.; Defrees, D. J.; Baker, J.; Stewart, J. J. P.; Head-Gordon, M.; Gonzalez, C.; Pople, J. A. *Gaussian 94*; Gaussian, Inc.: Pittsburgh, PA, 1995.

(22) Werner, H.-J.; Knowles, P. J.; Almlöf, J.; Amos, R. D.; Deegan, M. J. O.; Elbert, S. T.; Hampel, C.; Meyer, W.; Peterson, K.; Pitzer, R.; Stone, A. J.; Taylor, P. R.; Lindh, R. *MOLPRO*, version 96.1; University of Birmingham: Birmingham, 1996.

(23) (a) Hehre, W. J.; Ditchfield, R.; Pople, J. A. *J. Chem. Phys.* **1972**, *56*, 2257. (b) Hariharan, P. C.; Pople, J. A. *Theor. Chim. Acta* **1973**, *28*, 213. (c) Gordon, M. S. *Chem. Phys. Lett.* **1980**, *76*, 163.

(24) Møller, C.; Plesset, M. S. *Phys. Rev.* **1934**, *46*, 618.

(25) (a) Purvis, G. D.; Bartlett, R. J. *J. Chem. Phys.* **1982**, *76*, 1910. (b) Reghavachari, K.; Trucks, G. W.; Pople, J. A.; Head-Gordon, M. *Chem. Phys. Lett.* **1989**, *157*, 479.

(26) (a) Werner, H.-J.; Knowles, P. J. *J. Chem. Phys.* **1988**, *89*, 5803. (b) Knowles, P. J.; Werner, H.-J. *Chem. Phys. Lett.* **1988**, *145*, 514.

(27) Landau, L. D.; Teller, E. *Phys. Z. Sowjetunion* **1936**, *10*, 34.